

Provided for non-commercial research and education use.  
Not for reproduction, distribution or commercial use.



(This is a sample cover image for this issue. The actual cover is not yet available at this time.)

**This article appeared in a journal published by Elsevier. The attached copy is furnished to the author for internal non-commercial research and education use, including for instruction at the authors institution and sharing with colleagues.**

**Other uses, including reproduction and distribution, or selling or licensing copies, or posting to personal, institutional or third party websites are prohibited.**

**In most cases authors are permitted to post their version of the article (e.g. in Word or Tex form) to their personal website or institutional repository. Authors requiring further information regarding Elsevier's archiving and manuscript policies are encouraged to visit:**

**<http://www.elsevier.com/copyright>**

Contents lists available at [SciVerse ScienceDirect](http://www.sciencedirect.com)

# Journal of Non-Newtonian Fluid Mechanics

journal homepage: <http://www.elsevier.com/locate/jnnfm>

Short communication

## Emulsification using elastic turbulence

R.J. Poole\*, B. Budhiraja, A.R. Cain, P.A. Scott

School of Engineering, University of Liverpool, Brownlow Street, Liverpool L69 3GH, United Kingdom

### ARTICLE INFO

#### Article history:

Received 6 January 2012  
 Received in revised form 23 March 2012  
 Accepted 26 March 2012  
 Available online 10 April 2012

#### Keywords:

Elastic turbulence  
 Mixing  
 Emulsion

### ABSTRACT

In this short communication we show that so-called “elastic turbulence” – a chaotic flow driven by elastic stresses observable even in the absence of inertia – can be used to create emulsions from immiscible viscous liquids in a simple shear mixing device. In the absence of elasticity, but at identical viscosity ratio, Reynolds and Capillary numbers, no mixing is observed and the immiscible liquids remain separated. Elastic turbulence thus offers a unique pathway to create dispersions in viscous liquids at low Reynolds numbers in nominally shear-dominated flows.

© 2012 Elsevier B.V. All rights reserved.

### 1. Introduction

For Newtonian fluids, flows at very low Reynolds numbers ( $Re = \rho U h / \eta < 1$  where  $\rho$  is the fluid density,  $U$  a velocity scale,  $h$  a length scale and  $\eta$  the fluid viscosity) tend to remain laminar and steady. As a consequence mixing of fluids is inherently difficult to achieve efficiently for very viscous systems or liquid flows at small scales (e.g. microfluidics): they are essentially diffusion dominated. However, if a small amount of high molecular-weight polymer is added to water (or any Newtonian solvent), making the resulting solution viscoelastic, then fluid flows at arbitrarily small values of  $Re$  have been shown to exhibit “turbulent-like” characteristics such as randomly fluctuating fluid motion excited across a broad range of temporal and spatial scales [1–8]. These works show that highly-elastic fluids can undergo a series of flow transitions from viscometric laminar flow, to periodic flow, to apparently chaotic flow, and then to fully-developed elastic turbulence (ET) in conditions of negligible inertia ( $Re < 1$ ) in a range of flows; simple mixing devices based on torsional parallel plates [1,3,6], serpentine or wavy microchannels [2–5,8] and contraction–expansions [7]. At such low Reynolds numbers the flows are far from the inertially-driven turbulence observed for Newtonian fluids (which usually occurs at  $Re$  on the order of 1000 for internal flows) and are purely-elastic in nature. By “purely-elastic” we mean driven by non-linear elastic (normal) stresses that develop in flowing complex fluids and quantified using the ratio of elastic to viscous stresses: the Weissenberg number  $Wi = \lambda U / h$  where  $\lambda$  is the relaxation time of the complex fluid. Although the mixing effectiveness of the regime has been mentioned repeatedly [1–8] – at least in terms

of mixing of a passive scalar for example – little quantitative work has yet been carried out to assess this effectiveness outside of passive scalar mixing. Our aim here is to probe the possibility of using this “elastic” turbulence to create emulsions by vigorous mixing in a simple, nominally pure-shear, mixing device.

An emulsion contains liquid droplets dispersed in a second immiscible liquid (the continuous phase). The droplets are deformable, which imparts unique material properties to the emulsion, including shear-dependent viscosity and elasticity arising from surface tension [9]. The resulting rheology of the emulsion is directly related to the texture associated with numerous foods stuffs and personal care products (e.g. skin creams, mayonnaise, ice cream, etc.). The containment of liquids within droplets is also useful for controlling reactions, as the droplet interface acts as a membrane confining the contents. Using this concept, emulsions have been used to refine biochemical processes such as polymerase chain reaction for gene analysis and to control drug delivery rates [10]. All of these important emulsion properties depend strongly on the suspended droplet size and the uniformity of sizes within the sample. Although numerous high-energy emulsification methods exist such as atomization, sprays, and high-speed mixing they yield broad size distributions due to stochastic processes such as turbulent fluctuations [11]. At low Reynolds numbers, microfluidic technologies have emerged as a new route to the fabrication of uniform emulsions but the resulting throughputs are, without massive parallelisation, quite modest being on the order of 1  $\mu\text{l/s}$  per microfluidic cell [11]. In addition, for the limiting case of single (non-interacting) drops, the flow-field type plays a key role in determining whether break-up will even occur [12]. For pure shear flows, drop breakup is not possible above certain values of the viscosity ratio (dispersed/continuous  $\sim 4$ ) [13] or below certain values ( $< 0.005$ ) [14].

\* Corresponding author. Tel.: +44 151 794 4806.

E-mail address: [robpoole@liv.ac.uk](mailto:robpoole@liv.ac.uk) (R.J. Poole).

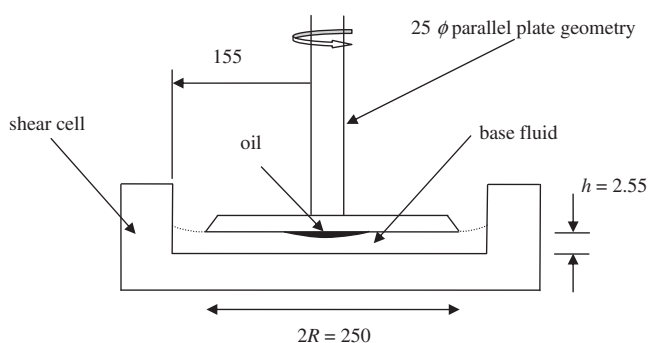


Fig. 1. Schematic of shear-cell arrangement (all dimensions in mm).

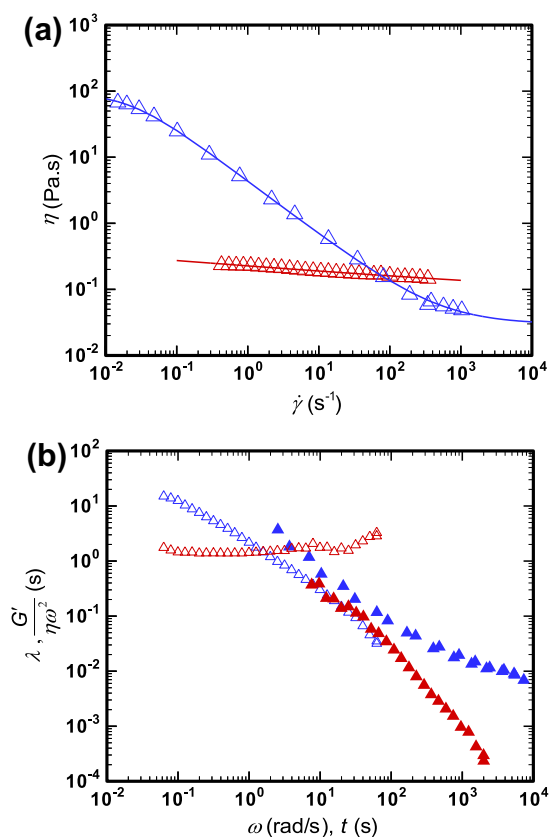


Fig. 2. Steady-shear rheology data. (a) Shear-viscosity versus shear rate (continuous line: Carreau–Yasuda fit) and (b) relaxation time determined from; closed symbols – first-normal stress data ( $\lambda = N_1/2\eta\dot{\gamma}^2$ ); open symbols – small amplitude oscillatory shear data ( $=G'/\eta\omega^2$ ). { $\Delta$ ,  $\blacktriangle$ : STF,  $\triangle$ ,  $\blacktriangle$ : BF}.

## 2. Details of mixing device and working fluids

To generate a simple nominally shear-dominated<sup>1</sup> mixing device – whilst ensuring excellent control of the applied torque or angular velocity – we modified a TA Instruments Rheolyst AR 1000N controlled-stress rheometer to incorporate a shear-cell arrangement as shown schematically in Fig. 1. A stainless-steel circular plate (25 mm in diameter) is connected to the control rod of the rheometer and the applied torque can be varied over a wide range (0.1  $\mu\text{N m}$ –100 mN m) and the resulting angular

<sup>1</sup> Of course, should elastic turbulence arise in the mixing device the flow will have strong extensional components and will no longer be pure-shear.

Table 1

Fluid properties for the base fluids (STF and BF) together with the immiscible oil.

Fluid	$\eta_0$ (Pa s)	$\lambda_0$ (s)	$\rho$ (kg/m <sup>3</sup> )	$\sigma$ (mN/m) <sup>a</sup>
STF	76.8	15	997	73
BF	0.238	1.7	1150	66
Squalene	0.04	–	858	28

<sup>a</sup> Measured on a Kruss Easy Dyne surface tensiometer using a Wilhelmy plate.

velocity measured. The base fluid (2 ml) is contained in a transparent shear-cell device whilst a small drop (0.2 ml) of the second (immiscible) liquid can be placed directly on top of the base fluid layer and then the plate lowered and subsequently rotated. Two different viscoelastic solutions, one shear-thinning solution and one of approximately constant viscosity (a so-called Boger fluid), were used in an attempt to separate out the effects of elasticity, shear thinning and viscosity ratio. The shear-thinning fluid (hereafter STF) was a polymer solution of 1% concentration by weight of a polyacrylamide, Separan AP 273E supplied by Floreger, in water. At this concentration the solution is concentrated as  $c/c^* \gg 1$  where  $c^*$  is the critical overlap concentration which is approximately 0.03% in water for this particular polyacrylamide. The Boger fluid (BF) was a 0.125% ( $c/c^* \sim 1$ ) concentration by weight of the same polymer in a glycerine/water solvent (90.875%/7.5%) with 1.5% salt added. All rheological measurements were performed using the TA controlled-stress rheometer in conjunction with a 60 mm 2° acrylic cone. Measurements comprised shear-viscosity, small amplitude oscillatory shear (SAOS) and first normal-stress difference ( $N_1$ ) variation with shear rate/angular frequency and are shown in Fig. 2a (viscosity) and b (SAOS and  $N_1$ ) respectively. The 1% aqueous solution strongly shear thins and the viscosity decreases by about four orders of magnitude from its zero shear rate value ( $\sim 80$  Pa s) whilst the Boger fluid's viscosity decreases by less than 25% from its zero shear rate value ( $\sim 0.24$  Pa s). Both shear viscosity data sets have been fit to the Carreau–Yasuda model [15] using the methodology outlined in [16] to allow us to estimate characteristic viscosity values at any shear rate. We estimate a shear-rate dependent relaxation time from the first normal-stress difference data (viz  $\lambda = N_1/2\eta\dot{\gamma}^2$ ) and the longest relaxation time ( $\lambda_0$ ) from SAOS measurements ( $=G'/\eta\omega^2$  in the limit of the angular frequency  $\omega$  tending to zero). For the immiscible oil we used a mineral oil – squalene supplied by Acros Organics – mixed with a small amount of an oil-soluble dye to aid visualisation (a paprika food dye supplied by Kelsec). Thus the oil drops appear bright yellow against the transparent base fluids. The important fluid properties for both the base fluids and the oil are listed in Table 1.

## 3. Scoping mixing experiments using a passive scalar

To determine the parameter space range (i.e.  $Re$  and  $Wi$ ) over which elastic turbulence was achievable in our mixing device with these base fluids we conducted some scoping experiments using a passive scalar (berlin blue dye). The results of these scoping experiments are shown for the Newtonian fluid in Fig. 3 and for a typical viscoelastic fluid run in the elastic turbulence regime Fig. 4. In the ET regime 2 min of mixing was sufficient to completely mix the dye (measured by colour intensity) whereas for a Newtonian fluid at the maximum Reynolds number used with the viscoelastic fluids ( $Re \approx 4$ ) no mixing was observed. In addition we were able to follow the time evolution of the angular velocity of the upper plate and within the ET regime this exhibited large RMS fluctuations – of the order of 10% of the mean – without dominant frequencies as shown in terms of apparent shear rate in Fig. 5.

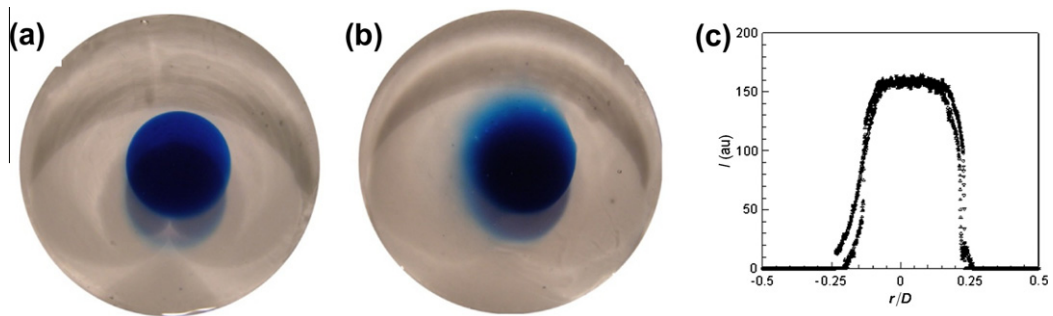


**Fig. 3.** Mixing of passive scalar (0.25 ml berlin blue dye) using shear cell with a Newtonian fluid (glycerine/water mixture),  $Re = 4$  (a)  $t = 0$  (before shear), (b)  $t = 120$  s (after shear), (c) colour intensity plot along horizontal mid plane ( $\nabla t = 0$  s,  $\Delta t = 120$  s).

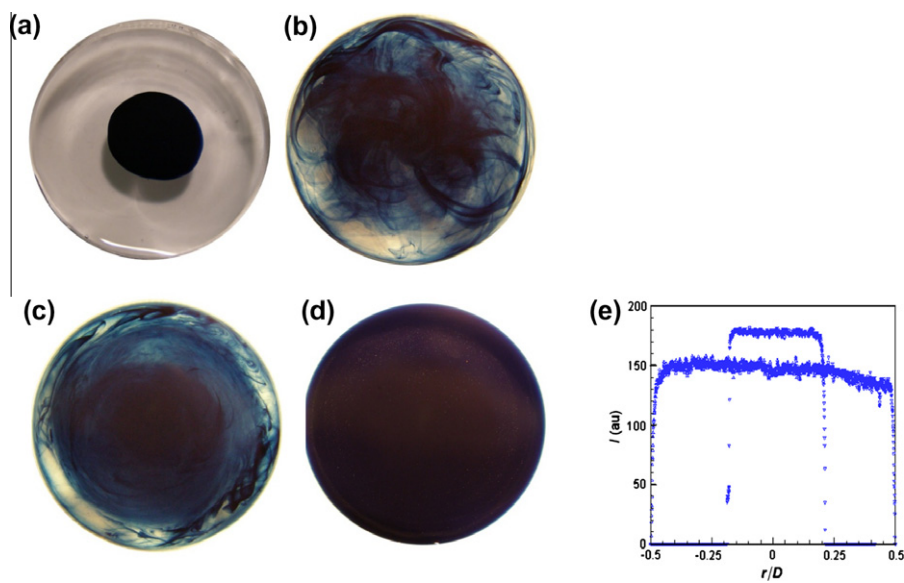


**Fig. 4.** Mixing of passive scalar (0.25 ml berlin blue dye) using shear cell with STF,  $Re_0 = 1 \times 10^{-2}$ ,  $Re = 4.6$ ,  $Wi = 5.2$ . (a)  $t = 0$  (before shear), (b)  $t = 30$  s, (c)  $t = 90$  s, (d)  $t = 120$  s (after shear), (e) colour intensity plot along horizontal mid plane ( $\nabla t = 0$  s,  $\Delta t = 120$  s).

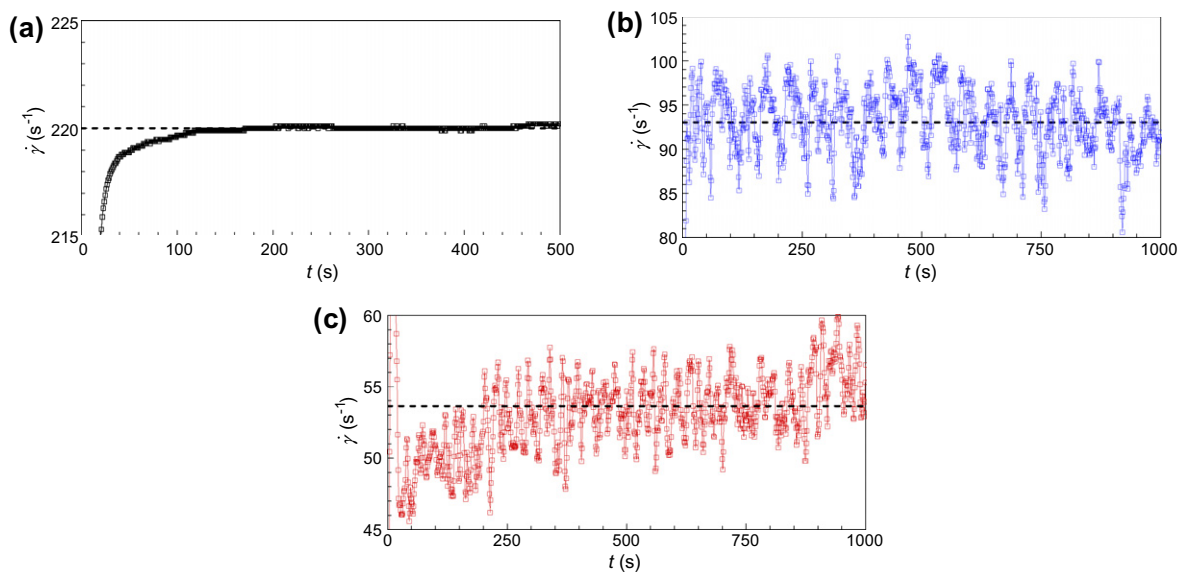


**Fig. 5.** Apparent shear rate variation with time for (a) Newtonian fluid  $Re = 0.11$ , (b) STF,  $Re_0 = 1 \times 10^{-2}$ ,  $Re = 4.6$ ,  $Wi = 5.2$ , (c) BF  $Re = 0.11$ ,  $Wi = 1.52$ .

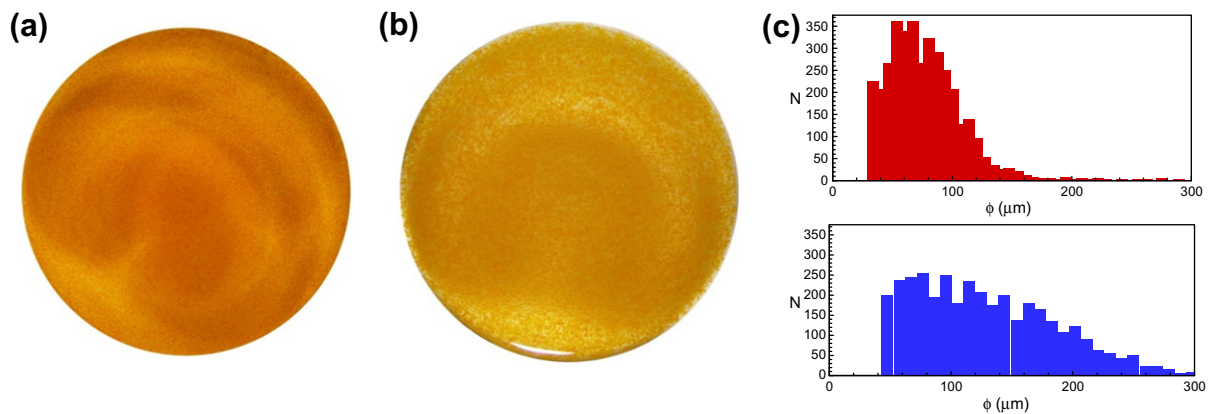


**Fig. 6.** Breakup of oil droplet (0.2 ml squalene) using shear cell with a (a) BF  $Re = 0.11$ ,  $Ca = 0.75$ ,  $Wi = 1.52$ ,  $t = 120$  s (after shear), (b) STF  $Re = 0.01$ ,  $Ca = 250$ ,  $Wi = 5.2$ ,  $t = 120$  s (after shear), (c) droplet size distribution for **Boger fluid** (upper panel) and **shear-thinning fluid** (lower panel).

#### 4. Emulsification using elastic turbulence

To investigate emulsification using ET we placed a 0.2 ml drop of the dyed oil on top of 2 ml of the continuous phase (base fluid), lowered the plate to a pre-determined gap ( $h = 2.55$  mm), and sheared for 2 min. Using a Newtonian glycerine solution of matching viscosity, density and interfacial tension to the Boger fluid (therefore fixing the viscosity ratio  $\eta_{oil}/\eta_0$ , the Reynolds number  $= \rho\omega R h/\eta_0$  and the Capillary number  $= \eta_0\omega R/\sigma$ ) the oil remained on the surface of the base fluid and no emulsification was achieved regardless of the applied shear rate (indeed even up to Reynolds numbers an order of magnitude greater than that used to create ET). These observations were found to be independent of the time of shearing: experiments of 10 min duration gave essentially the same results. In marked contrast when the experiments were repeated with the viscoelastic base fluids under ET conditions, good emulsions were created for both the BF (a typical result is shown in Fig. 6a) and the STF (Fig. 6b). No results are shown for the Newtonian base fluid due to the absence of any emulsification. To quantify the effectiveness of the emulsification we measured the droplet size distribution using image processing software of magnified images (Fig. 6c). Despite the large differences in viscosity ratio between the two base fluids (1000 times greater for the BF compared to the STF) and capillary numbers (approximately 30 times greater for the STF) the Sauter mean diameter ( $\phi$ ) is the same order ( $\sim 100$   $\mu\text{m}$ ) in both cases. (We note, however, that if a characteristic viscosity is estimated for the STF, based on a characteristic shear rate of  $\omega R/h$  for example, the viscosity ratio and capillary number becomes of the same order as the BF as  $\eta_{CH} \sim 0.0025\eta_0$ ). Slight quantitative differences in the mean droplet diameters in each case – and more noticeably in the larger standard deviation for the STF – are probably ascribable to the significantly different rheology for each fluid (strong shear-thinning for the STF). The sharp cut-off observable in the droplet diameter data below about 40  $\mu\text{m}$  represents the minimum resolution of the image processing software: droplets below this diameter could not be quantified. Finally the addition of a small amount (0.2% w/w) of a surfactant (sodium dodecyl sulphate) to the oil to reduce its interfacial tension (viscosity remained unaltered but surface tension reduced by 15%) had almost no effect on the droplet size or distribution confirming that the driving mechanism for the emulsification was elastic turbulence.

#### Acknowledgements

We would like to thank Dr. Harry Barraza (Unilever Research Port Sunlight), Prof. Manuel Alves (U. Porto) and Dr. Alexander Morozov (U. Edinburgh) and the anonymous reviewer for helpful comments. We would also like to thank Dr. Volfango Bertola (U. Liverpool) for help with the surface tension measurements.

#### References

- [1] A. Groisman, V. Steinberg, Elastic turbulence in a polymer solution flow, *Nature* 405 (2000) 53–55.
- [2] A. Groisman, V. Steinberg, Efficient mixing at low Reynolds numbers using polymer additives, *Nature* 410 (2001) 905–908.
- [3] A. Groisman, V. Steinberg, Elastic turbulence in curvilinear flows of polymer solutions, *New J. Phys.* 6 (2004) 29–48.
- [4] T. Burghelca, E. Segre, I. Bar-Yosef, A. Groisman, V. Steinberg, Chaotic flow and efficient mixing in microchannel with a polymer solution, *Phys. Rev. E* 69 (2004) 066305.
- [5] T. Burghelca, E. Segre, V. Steinberg, Role of elastic stress in the statistical and scaling properties of elastic turbulence, *Phys. Rev. Lett.* 96 (2006) 214502.
- [6] B.A. Schiameberg, L.T. Shereda, H. Hu, R.G. Larson, Transitional pathway to elastic turbulence in torsional, parallel-plate flow of a polymer solution, *J. Fluid Mech.* 554 (2006) 191–216.
- [7] H.Y. Gan, Y.C. Lam, N.T. Nguyen, A polymer-based device for efficient mixing of viscoelastic fluids, *Appl. Phys. Lett.* 88 (2006) 224103.
- [8] F.C. Li, H. Kinoshita, X.B. Li, M. Oishi, T. Fujii, M. Oshima, Creation of very-low-Reynolds-number chaotic fluid motions in microchannels using viscoelastic surfactant solution, *Exp. Therm. Fluid Sci.* 34 (2010) 20–27.
- [9] L.L. Schramm, *Emulsions, Foams, and Suspensions: Fundamentals and Applications*, Wiley-VCH, 2005.
- [10] A.D. Griffiths, D.S. Tawfik, Miniaturising the laboratory in emulsion droplets, *Trends Biotechnol.* 24 (2006) 395–402.
- [11] G.F. Christopher, S.L. Anna, Microfluidic methods for generating continuous droplet streams, *J. Phys. D: Appl. Phys.* 40 (2007) R319.
- [12] H.A. Stone, Dynamics of drop deformation and breakup in viscous fluids, *Annu. Rev. Fluid Mech.* 26 (1994) 65–102.
- [13] G.I. Taylor, The formation of emulsions in definable fields of flow, *Proc. Roy. Soc. Lond. Ser. A* 146 (1934) 501–523.
- [14] H.J. Karam, J.C. Bellinger, Deformation and breakup of liquid droplets in a simple shear field, *I&EC Fund.* 7 (4) (1968) 576–581.
- [15] K. Yasuda, R.C. Armstrong, R.E. Cohen, Shear flow properties of concentrated solutions of linear and star branched polystyrenes, *Rheol. Acta* 20 (1981) 163–178.
- [16] M.P. Escudier, I.W. Gouldson, A.S. Pereira, F.T. Pinho, R.J. Poole, On the reproducibility of the rheology of shear thinning liquids, *J. Non-Newt. Fluid Mech.* 97 (2001) 99–124.